

# On the extension of a laser-Doppler velocimeter to the analysis of oscillating flames

by

E.C. Fernandes and M.V. Heitor

Instituto Superior Técnico

Mechanical Engineering Department

Av. Rovisco Pais, 1049 - 001 Lisboa; Portugal

## ABSTRACT

A measuring system based on a laser-Doppler velocimeter has been extended to include time-resolved temperature and sound pressure measurements, in order to allow the analysis of unsteady reacting flows. Measurements are reported for open recirculating flames oscillating with of a predominant frequency in the range of 265-275 Hz, and have been obtained for velocity data ready signals up to 12.5 kHz, allowing the time-resolved representation of vectors of turbulent heat flux along a typical cycle of oscillation. The results were obtained for flames stabilised in the wake of a bluff-body located on a velocity acoustic antinode. The acoustic resonance process driven by coherent structures along the reacting shear layer results in appreciable spatial and temporal deformations of the reacting flow field, which generate large periodic fluctuations in streamline curvature. This is accompanied by large fluctuations in the axial and radial velocity components of the flow as shown in figure 1. Together with the unsteady nature of the turbulent temperature field this results in a process of turbulent heat flux exhibiting a time sequence of gradient and non-gradient characteristic modes.

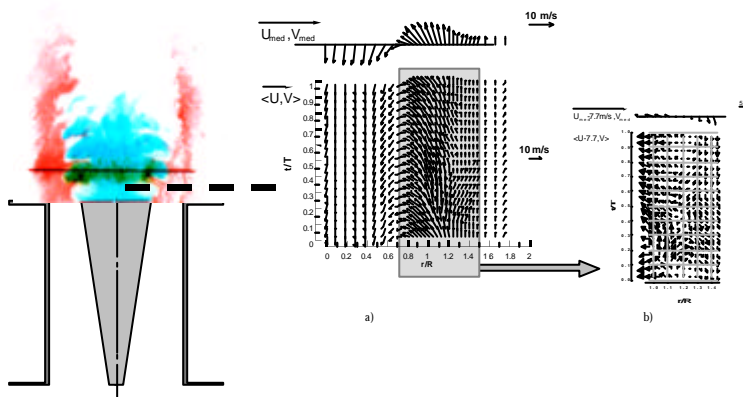


Fig. 1. Time evolution of the phase averaged velocity vectors at axial station  $z/R=0.58$  for an unsteady flame

a) Time evolution of phase averaged velocity vectors

b) Time evolution of phase averaged velocity vectors after the application of a “Galilean transformation” to subtract a vortex convection axial velocity of  $7.7 \text{ m/s}$

## 1. INTRODUCTION

Pulsating flows have been the subject of many investigations covering a wide range of situations, such as: acoustics (Herzog et al., 1996), heart valves (Hirt et al., 1996), in-cylinder combustion chambers (e.g. Liou and Santavicca, 1985, Witze, 1984), unstable shear layers (Hussain and Zaman, 1980), pulsed flames (e.g. Lovett and Turns, 1993), pulse combustors (Keller and Saito, 1987) and afterburners (Heitor et al., 1984, Gutmark et al., 1991 and Sivasegaram and Whitelaw, 1987). Different diagnostic techniques have been used, depending on the purpose of the investigation and on the nature of the flow. For example, the quantification of heat release in pulsed flames has been made through PLIF of OH and CH concentrations (e.g. Gutmark et al., 1989). The velocity field has been measured with hot-wire velocimetry in isothermal flows (e.g. Hussain and Zaman, 1980 and Kya and Sasaki, 1985), and with laser velocimetry in oscillating flows (Dec et al., 1991). Temperature measurements have been reported with TLAF technique (Dec and Keller, 1990) and with fine bare-wire thermocouples (e.g. Ishino et al., 1996). High speed Schlieren cinematography has also been used (e.g. Keller et al., 1982 and Ganji and Sawyer, 1989) to record the structure of the reacting flowfield, together with phase average digital photography as a non-expensive visualization technique (Chao et al., 1991).

While most of the works mentioned above report the acquisition of single variables, other have attempted to correlate multiple signals (e.g. Lang and Vortmeyer, 1987; Keller, 1995), or to control the process of vortex shedding associated with unsteady flames (e.g. Schadow and Gutmark, 1992), but in general there is a need of reliable data on the coupling mechanisms between pressure, velocity and heat release fluctuations in order to better understand the onset of combustion induced oscillations. In this context, this paper analyzes the extension of a conventional laser velocimeter to the simultaneous measurement of the time-resolved fluctuations of velocity, pressure and temperature, in unsteady reacting flows. The system was developed in order to characterize natural unsteady flames such as those presented in figure 1 downstream of two distinct flame holders, but both of them driven by similar large-scale structures that develop along the shear layer and modulate the process of heat release. The following paragraphs describe the experimental method, including the data acquisition system, and present sample results obtained in the reacting shear layer of the flames of figure 1.

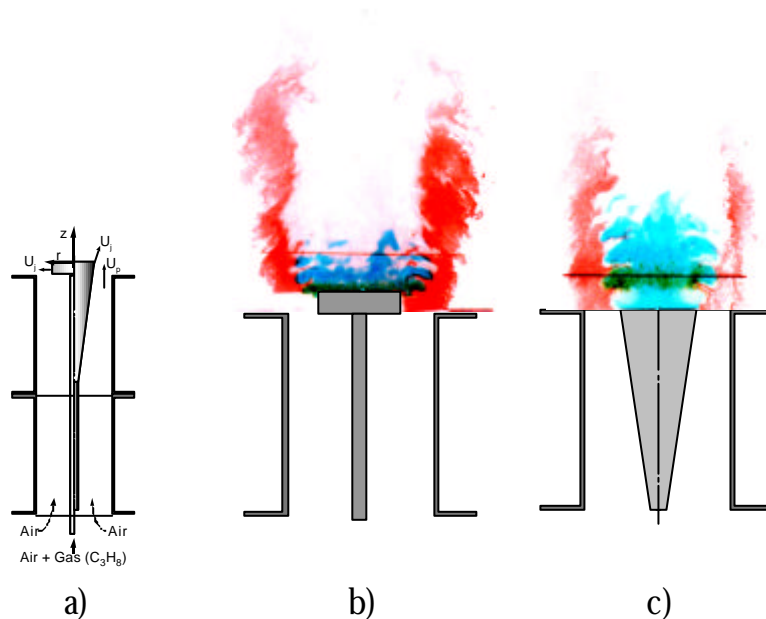


Fig. 2. Schematic diagram of flame holders and image of flames studied.

- a) Diagram of flame holders, conical and cylindrical, with identification of principal variables
- b) Short time film exposure (1/8000sec) of an unsteady flame - Flame A (cylindrical burner)
- c) Short time film exposure (1/8000sec) of an unsteady flame - Flame B (conical burner)

## 2. EXPERIMENTAL METHOD and PROCEDURES

### 2.1 The Flames considered

The flames considered throughout this paper were stabilized downstream flameholders located at the end of a 0.52m long tube (see figure 2a), which was placed on the top of a plenum chamber (for details see Fernandes, 1998). The resulting flame, burning a mixture of propane and air, is open to the atmosphere, and offers the advantage of easy access to the techniques described below.

For the range of unsteady conditions considered here, the spectrum of the pressure fluctuations in any location of the pipe wall is associated with the excitation of a predominant frequency in the range of 265-275 Hz (Fernandes, 1998), which is associated with a longitudinal standing half-wave. The flames are then located in a velocity antinode and the resulting time-resolved characteristics are described below. Both flames are also characterised by a sound pressure level of about 110dB. The analysis consider boundary conditions of  $\phi_1 = 8$ ,  $U_j = 8.8\text{m/s}$  and  $U_p = 2.9\text{m/s}$  for the Flame A presented in figure 2b and  $\phi_1 = 6$ ,  $U_j = 15\text{m/s}$  and  $U_p = 3.4\text{m/s}$ , for Flame B of figure 2c.

### 2.2 Experimental Techniques

Figure 3 shows schematically the various experimental techniques used throughout this work. Time-resolved velocity information was obtained with a laser-Doppler velocimeter, which comprised an Argon-Ion laser operated at a wavelength of 514.5 nm and a power of around 1W. A fiber optic (DANTEC) was used to guide the beam to an optical unit arranged with a two beam system with sensitivity to the flow direction provided by light-frequency shifting from a Bragg cell at 40MHz, a 310 mm focal length transmission lens, and forward-scattered light collected by a 300 mm focal length lens at a magnification of 1.0. The half-angle between the beams was  $5.53^\circ$  and the calculated dimensions of the measuring volume at the  $e^{-2}$  intensity locations were 2.3 and 0.219 mm. The output of the photomultiplier was mixed with a signal derived from the driving frequency of the Bragg cell and the resulting signal processed by a commercial frequency counter (DANTEC 55296) interfaced with a 16-bit DSP board. Measurements were obtained with the laser beams in the horizontal and vertical planes and by traversing the control volume along the horizontal and vertical directions to allow the determination of the axial, U, and radial, V, time-resolved velocities, respectively.

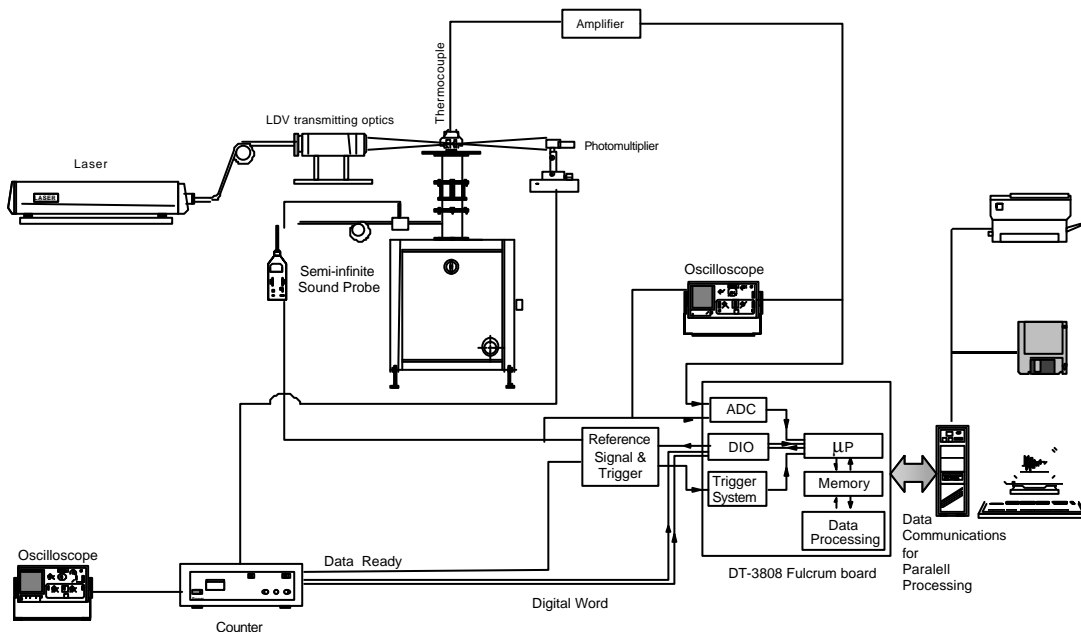


*Fig. 3. Schematic drawing of experimental apparatus with identification of the instrumentation used for simultaneous measurements of velocity-temperature-pressure in unsteady flows. Source: Fernandes (1998).*

Temperature measurements were obtained making use of fine-wires thermocouples, with 38  $\mu$ m in diameter, made of Pt/Pt-13%Rh. The thermocouple output signal was digitally compensated from thermal inertia, following the procedure first outlined by Heitor et al. (1985), but optimised and used by Ferrão and Heitor (1998) and Caldeira-Pires and Heitor (1998) in premixed and non-premixed flames, respectively. The related uncertainties are quantified elsewhere (see for example Ferrão and Heitor, 1998 and Fernandes, 1998) and shown not to be higher than 60K for time-averaged values at the maximum temperature obtained in the open flames considered here, and up to 15% for the variance of the temperature fluctuations. In fact, the largest random error incurred in the values of temperature-velocity correlation, as high as 15%, are due to the spatial separation of the measurements locations of the temperature and velocity because of the thermocouple junction must lie outside the measuring control volume of the laser velocimeter (e.g. Caldeira-Pires and Heitor, 1998, Ferrão and Heitor, 1998).

The sound intensity signal from the flame was acquired with a semi-infinite probe with a flat response up to 1kHz. The system is based on a free-field condenser microphone (B&K 4130) and a pre-amplifier (B&K 2130) with a flat response over a frequency band of 20Hz to 10kHz (Fernandes, 1998). This signal was used as a reference signal for data acquisition and post-process. The instantaneous pressure fluctuations correspond to signals measured at middle of the pipe, where the amplitude of the pressure fluctuations is maximum.

The complete measuring system was mounted in a three-dimensional traversing unit, allowing an accuracy of the measuring control volume within  $\pm 0.25$ mm.

### **2.3 Data Acquisition and System Control**

The Doppler digital word and the two scalar signals, pressure and temperature, were acquired simultaneously and post-processed making use of a microprocessor, Texas Instruments-TMSC320C40, which also controls the LDV counter and the phase encoder box. The scalar signals were digitised with a sample-and-hold 16bits A/D converter at a rate of 40kHz/channel and stored in a circular memory buffer. The digital Doppler signal (8 bits mantissa and 4 bits exponent) is acquired with a dynamic digital input port.

According to the scheme presented in figure 4, the system initiates the DSP internal timer counter after a initial start flag is set to a logic value "true" on the transition of the pressure signal from positive to negative, controlled by the phase encoder box. Meanwhile, the process of analogue acquisition, which is running at a rate of 40kHz/channel is used to save temperature and pressure data into a circular memory by the action of an internal DMA co-processor. Then, for each LDV burst event, the sequence of actions is as follows:

- the time at which the burst event occurs is stored
- the DMA pointer of the exact location in the circular buffer at that time is stored
- the DSP external trigger is set to a logic value of "true", causing the counter to be stopped after 100ns
- the digital word is read and converted into velocity
- the pressure signal value at that time is read from the circular buffer
- two points before and after the temperature value at that time is also read from the circular buffer
- time, velocity, pressure and temperature are transferred to vector memory and calculations of the time derivative of temperature are made.

The process is concluded after a total acquisition time,  $T_{acq}$ , is concluded, following which all internal control variables are reset. The cycle repeats until a total population size of about N points (10240 or 20480) is acquired. For the measurements presented in this paper, the complete system ran up to 12.5kHz of data ready signals, with the delay of the board to the data ready signal less than 100ns, and with the window resolution between velocity and scalars less than 1/40kHz.

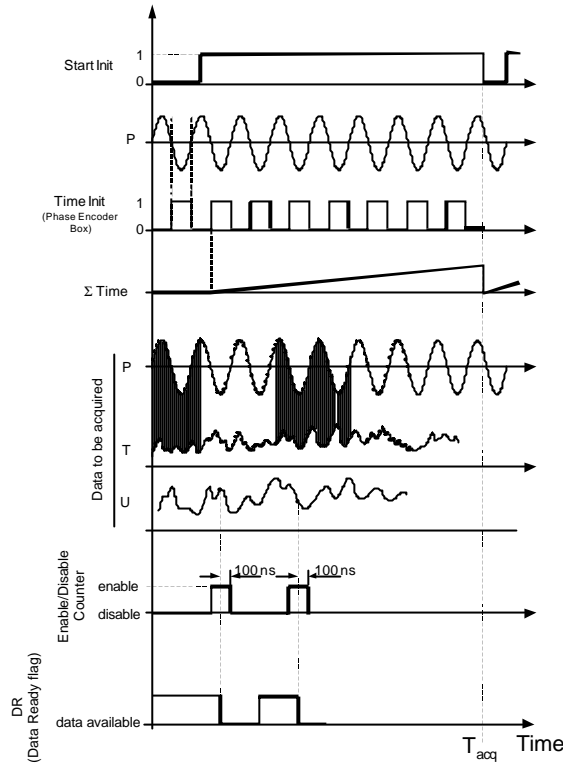


Fig. 4. Temporal diagram for simultaneous measurements of velocity (random data), pressure and temperature (continuous signals) in unsteady flows, and for hardware control

### 3. RESULTS AND DISCUSSION

Figure 5 show results of velocity acquired with different data rates and of temperature (non-compensated signal) acquired with a constant data rate of 40kHz. Both signals were obtained for unsteady Flame A and show a quasi-periodical variation in time. The amplitude and frequency are variable in time and, together with the random nature of the Doppler signals, imply that the detailed analysis of the time-resolved local flame characteristics has required the development of a purpose-built system for frequency analysis and phase-averaging, as discussed in the following paragraphs.

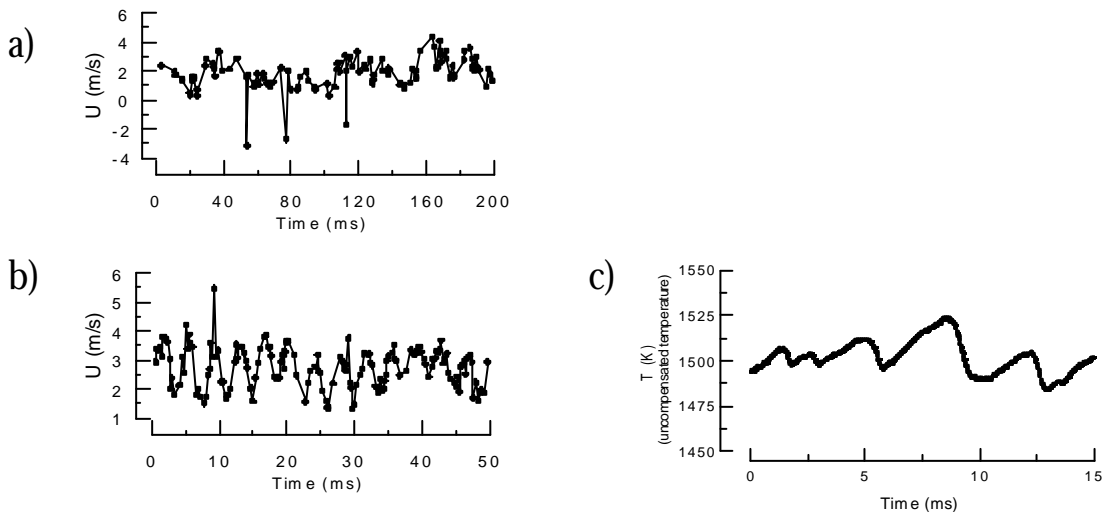


Fig. 5. Sample of time-resolved measurements of velocity and temperature in an unsteady flame oscillating with a frequency of about  $275\text{Hz} \pm 1.24\text{Hz}$

- a) Axial velocity time series acquired with a mean data rate of  $700\text{Hz}$  – (Flame A,  $r/R=0.92$ ,  $z/R=0.53$ )
- b) Axial velocity time series acquired with a mean data rate of  $3500\text{Hz}$  – (Flame A,  $r/R=0.92$ ,  $z/R=0.53$ )
- c) Temperature time series acquired with a constant data rate of  $40\text{kHz}$  – (Flame B,  $r/R=1.24$ ,  $z/R=0.58$ )

### 3.1 Frequency Analysis

Although various weighting methods have been proposed to correct for velocity bias effects (e.g. Durst et al., 1981), no corrections were applied to the measurements reported here. The systematic errors that could have arisen were minimised by using high data acquisition rates in relation to the fundamental velocity fluctuation rate, as suggested for example by Erdman and Tropea (1981). This could be easily achieved because the rate of naturally occurring particles was sufficiently high for the flow conditions considered here.

Spectral analysis of LDV signals was carried out by resampling the time series after a linear interpolation with minimum interval time given by the mean data rate.

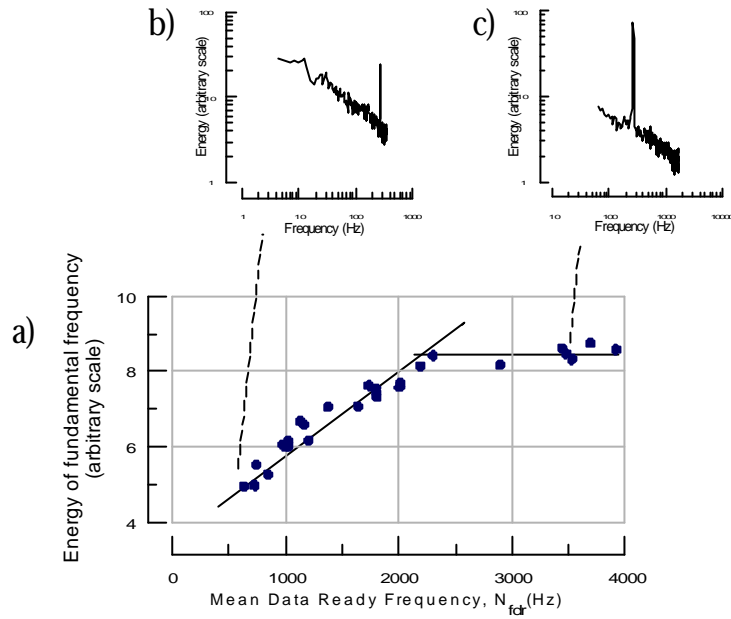


Fig. 6. Spectral analyses of LDV data as a function of mean data rate for typical unsteady flame conditions (Flame A) characterised by a fundamental frequency of  $1/T_{osc} = 265 \pm 2.4$  Hz

- a) Energy of fundamental frequency as a function of mean data rate
- b) Velocity spectrum for  $N_{fdr} = 700$  Hz ( $N_{fdr}T_{osc} = 2.64$ )
- c) Velocity spectrum for  $N_{fdr} = 3500$  Hz ( $N_{fdr}T_{osc} = 13.2$ )

Figure 6 show results of peak amplitude at 265 Hz as a function of the data ready frequency,  $N_{fdr}$ , of the counter for a typical location in the reacting shear layer studied through this work. The measurements were obtained for conditions corresponding to data ready signals associated with each new Doppler burst. The results show that the predominant flow frequency of 265 Hz could be identified in the spectra of the velocity fluctuations for any data rate, although the energy associated with this frequency (in a band of  $\pm 2.4$  Hz) is independent of that rate only for  $N_{fdr} > 2.3$  kHz. This agrees with the conditions given by, for example, Adrian and Yao (1989) for which the output of the counter yields a satisfactorily spectral analysis for the frequency range considered here.

Spectral and temporal analysis of temperature time-series requires a compensation procedure as outlined by Ferrão and Heitor (1998) because of the thermocouple time-lag. In figure 7a the results are those of original temperature time-series, as acquired by the thermocouple and the corresponding digitally compensated time series. While there are significant differences in the amplitude domain, as also reported by the results of figure 7b, the phase compensation is quite insensitive to the numerical compensation because the dominant frequency (275 Hz) is quite above 100 Hz, as already pointed out by Lovett and Turns (1993) and further discussed by Fernandes (1998).

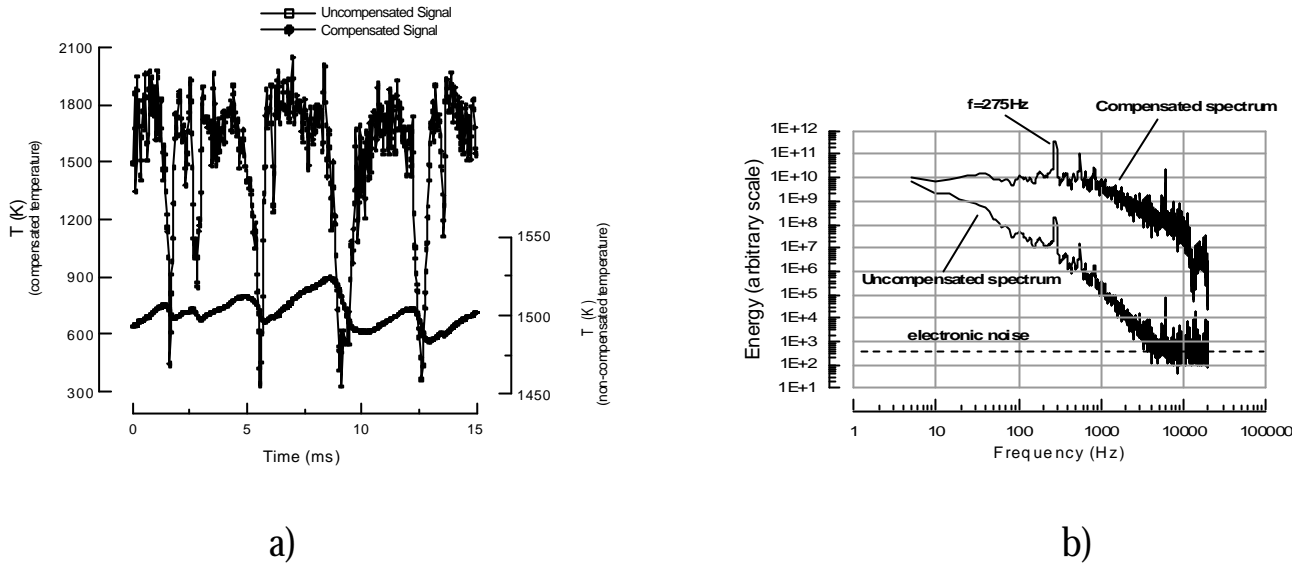


Fig. 7. Results of digital compensation of thermocouple thermal inertia obtained for Flame A at  $z/R=0.58$ ,  $r/R=1.24$ .

- Comparison of typical non-compensated and compensated temperature time-series for a narrow time window of 15ms.
- Comparison of typical non-compensated and compensated temperature spectra

### 3.2 Phase-Averaging Process

Important sources of uncertainty that may arise when measurements are taken in periodic flows include “*cycle-to-cycle*” variations, *temporal-gradient bias* and *phase bias*, and which can affect the phase-averaging process. The former are typically associated with in-cylinder flows in combustion engines, due to intake and exhaust process. To quantify this type of uncertainty, data acquisition and processing should include FFT analysis to separate the periodic from the non-periodic component of the flow (Dimopoulos et al., 1996). The *temporal-gradient bias* arises when phase-locked ensemble-averaging methods are employed to process signals with large temporal gradients, over a finite time window. The phase bias problem was addressed, for example, by Hussain and Zaman (1980) and consists essentially in a “jitter” effect, i.e. phase variations that generates virtual fluctuations. In the case reported here, this problem may arise through the pressure fluctuations, since this variable is used as a reference signal and is not strictly constant, therefore contaminates the velocity and temperature signals. In the work presented here, these uncertainties were quantified and shown not to affect the results.

A main question that arises in the detailed analysis of the present periodic flames is related with the adequacy of the pressure signal emitted by naturally pulsed flames as a reference signal for velocity measurements and for the phase-averaging process. This is because frequency variations can affect the velocity signal, creating a virtual turbulent fluctuation that is known to be a function of acquisition time (Fernandes, 1998). While pressure signals are only used as absolute reference signals, the observed spread of data points can have a significant influence on the associated velocity, affecting in this case the velocity rms. Analysis have shown that the influence of frequency uncertainties on the accuracy of the acquired data can be minimized if the acquisition time  $T_{acq}$  (see figure 4) is kept lower than 40ms (Fernandes, 1998). However, the choice of this value can have a dramatic influence on the total time spent to acquire  $N$  data points, as can be observed in the results of figure 8. This figure shows results obtained simulating a constant data rate of LDV triggers of about 6kHz, which represent the time taken by the hardware-software to perform all step functions specified in figure 3, in obtaining 10240 data points. Here a value of 40ms was chosen to allow a statistically independent sample of, at least, 10240 data points (Yanta and Smith, 1978), as shown in figure 9.



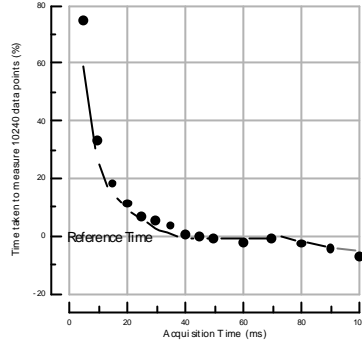


Fig. 8. The influence of maximum exposure time (before reset of the hardware) on the total time taken to acquire 10240 data points

Figure 9 shows a “partial phase-averaged” time series of pressure, axial and radial velocity and non-compensated temperature obtained with an average data rate of 200Hz for the unsteady Flame B, following the procedure outlined in previous paragraphs. The unsteadiness of the flow field is clearly visualised in the “partial” phase-averaged signal, and is associated with the temporal evolution of the turbulent or incoherent fluid motion. This is clearly identified through phase-resolved measurements of velocity, temperature and pressure obtained under periodic oscillations, figure 9b-c, which were statistically analysed following the decomposition proposed by Hussain and Reynolds (1970). For a generic variable  $\gamma$ :

$$\gamma(t) = \bar{\gamma} + \tilde{\gamma}(t) + \gamma'(t),$$

where  $\gamma(t)$  is the instantaneous value,  $\bar{\gamma}$  is the long time average mean,  $\tilde{\gamma}$  is the statistical contribution of the organised wave, and  $\gamma'(t)$  is the instantaneous value of turbulent fluctuations. An ensemble average over a large number of cycles yields (Hussain and Reynolds, 1970 and Tierderman et al. 1988):

$$\langle \gamma \rangle (t) = \bar{\gamma} + \tilde{\gamma}(t) \quad ; \quad \langle \sqrt{g'^2} \rangle (t_i \pm \Delta t) \equiv \langle g_{rms} \rangle = \sqrt{\frac{\sum_{i=1}^N (g'(t_i \pm \Delta t) - \langle g \rangle_{med}^*)^2}{n-1}}$$

The phase interval,  $t_i \pm \Delta t$ , was chosen to be  $18^\circ/360^\circ$ , to minimise the influences of the phase averaging window size on the determination of turbulence quantities in unsteady turbulent flows, as discussed by Zhang et al. (1997). In addition, the average values at each window,  $\langle \gamma \rangle_{med}^*$  were determined using a best-fit polynomial of first degree to minimise the temporal bias (Fernandes, 1998).

### 3.3 Sample Results

Figure 10 presents the temporal evolution of  $\langle U, V \rangle$ ,  $\langle U_{rms} \rangle$ ,  $\langle V_{rms} \rangle$ ,  $\langle T \rangle$ ,  $\langle T_{rms} \rangle$  and velocity-temperature correlation, for the region  $0.9 < r/R < 1.5$  at  $z/R = 0.58$ . The ensemble-average velocity vectors are presented in figure 10a) together with mean vectors distribution. Together, they identify a central recirculation zone that is quite insensitive to the natural oscillations that are occurring in the shear layer. The large deflections of the velocity vectors in this region are due to the presence of coherent structures, as observed in the images of figure 2b-c, and confirmed by the velocity vectors of figure 10b. These velocity vectors were obtained with a *Galelian transformation* where a velocity of 7.7m/s, due to the vortex convection, was subtracted from the axial velocity component. The velocity vectors are not constant in time and identify the passage of a vortex  $t/T = 0.5$  and  $r/R = 1.2$  through the presence of a temporal “saddle point”. This unsteadiness is accompanied by a singular distribution of turbulent kinetic energy, as shown in figure 10-c1, which double peaks, with the time evolution of velocity fluctuations as in figures 10c2 and 10c3. The results confirm the high level of velocity fluctuations near the vortex core, where the radial gradient of axial velocity is positive and maximum.

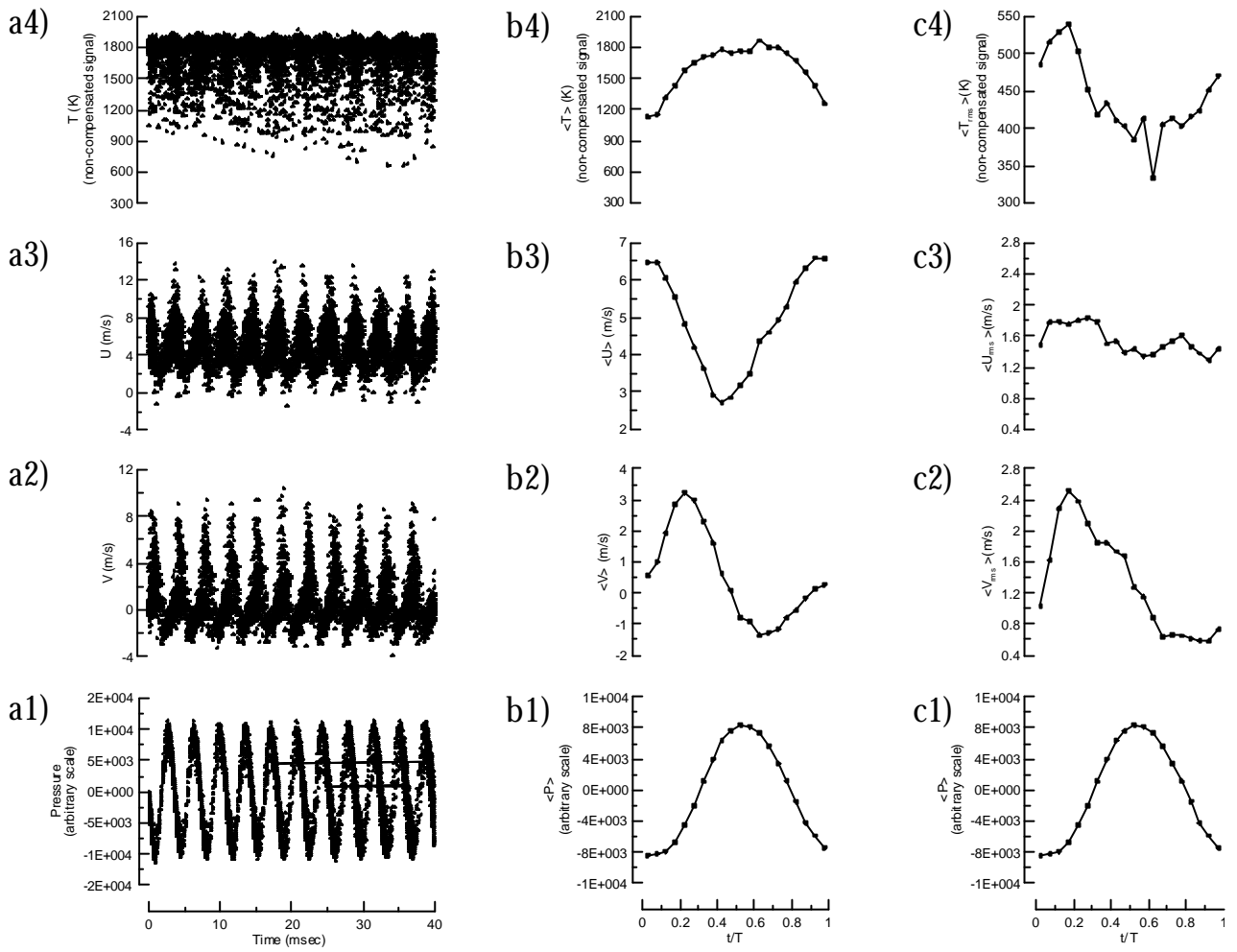


Fig. 9. Typical data reduction process from acquired signals to an evolution within a period of oscillation, for the unsteady Flame B, at  $z/R=0.58$ ,  $r/R=1.24$

a1-a4) Partial phase-averaged signals, as acquired by the system, of pressure a1), radial velocity a2), axial velocity component a3) and temperature a4).

b1-b4) Phase averaged results of mean pressure, axial and radial velocity components and compensated temperature signals

c1-c4) Phase averaged results of velocity and temperature turbulent fluctuations

The temperature characteristic profiles, figure 10d1-d3), show a rather complex nature, in that they suggest two typical high temperature regions, for  $r/R < 1.04$  and at  $r/R = 1.2$ . Both maxima temperature is of about 1800K while the lowest temperature measured is of the order of 800K. The phase averaged evolution of temperature, figure 10d2, denotes the influence of large vortical structures on the heat release in the shear layer. The rms of temperature fluctuations, figure 10d3), shows values in the range of

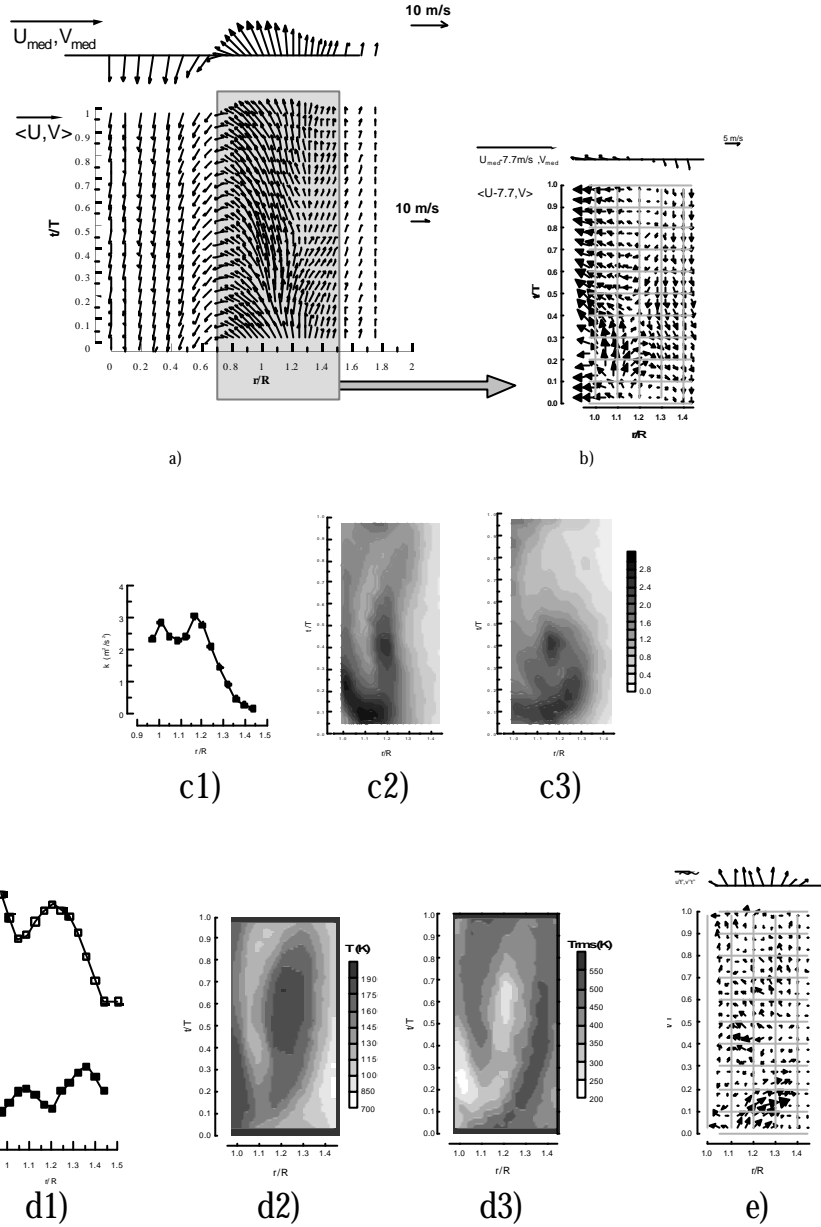


Fig. 10. Time evolution of the phase averaged velocity vectors, temperature characteristics and velocity-temperature correlation at axial station  $z/R=0.58$  for the Flame B

- c) Time evolution of phase averaged velocity vectors
- d) Time evolution of phase averaged velocity vectors after the application of a “Galilean transformation” to subtract a vortex convection axial velocity of 7.7m/s
- e) Turbulent velocity characteristics
  - c1) Radial evolution of mean turbulent kinetic energy
  - c2) Time evolution of  $\langle U_{rms} \rangle$
  - c3) Time evolution of  $\langle V_{rms} \rangle$
- f) Turbulent temperature characteristics
  - d1) Radial evolution of mean and turbulent fluctuations of temperature
  - d2) Time evolution of  $\langle T \rangle$
  - d3) Time evolution of  $\langle T_{rms} \rangle$
- e) Time evolution of  $\langle u''t'', v''t'' \rangle$  correlation

200K to 500K, in a way which is consistent with the findings of figure 10d2) in the sense that the maximum temperature fluctuations, at each time instant, occurs close to the regions where the instantaneous mean temperature exhibit a higher radial gradient.

Figure 10e) presents new information, in that it quantifies the temporal evolution of vectors of turbulent heat flux along a cycle of oscillation. These vectors represent the exchange rate of reactants responsible for the phenomenon of flame stabilisation and are high in regions associated with large temperature gradients. Previous results in the literature for steady recirculating flames (e.g. Fernandes et al., 1994, Hardalupas et al., 1996, Duarte et al., 1997) have shown the occurrence of zones of non- and counter-gradient diffusion of heat, which have been explained in terms of the interaction between gradients of mean pressure and density fluctuations. The present results provide new evidence of this interaction in oscillating flames, which is associated with periodic fluctuations in flame curvature. In general, the results quantify the periodic ignition of large-scale reaction zones, which drive the combustion-induced oscillations reported in this paper.

#### 4. SUMMARY

Optical and probe techniques are used to analyse the coupling mechanism between pressure, velocity and temperature fluctuations typical of pulsed flames, through the combination of laser velocimetry, digitally-compensated thermocouples and a probe microphone. The system is based on a digital signal microprocessor and is shown to run up to 12.5 kHz of data ready velocity signals, allowing the time-resolved representation of vectors of turbulent heat flux along a typical cycle of oscillation. The detailed results obtained along the oscillating reacting shear layer show time sequences of zones characterised by gradient and non-gradient turbulent heat flux, which are structurally similar to previous results reported in the literature for steady recirculating flames.

#### REFERENCES

- Adrian, R.J. and Yao, C.S. (1989). "Power Spectra of Fluid Velocities Measured by Laser-Doppler Velocimetry. ASME, Winter Annual Meeting, Miami Beach, Florida, November 17-22, 1995.
- Caldeira-Pires, A. and Heitor, M.V. (1998). "Temperature and Related Statistics Measurements in Turbulent Jet Flames", *Experiments in Fluids*, **24**, pp. 118-129.
- Chao, Y.C., Jeng, M.S. and Han, J.M. (1991). " Visualization of Image Processing of an Acoustically Excited Jet Flow", *Experiments in Fluids*, **12**, 29-40
- Dec, J.E. and Keller, J.A. (1990). "Time Resolved Gas Temperature in the Oscillating Turbulent Flow of a Pulse Combustor Tail Pipe", *Comb. And Flame*, **80**, pp.358-370
- Dec, J.E., Keller, J.O. and Hongo, I. (1991). "Time-Resolved Velocities and Turbulence in the Oscillating Flow of a Pulse Combustor Tail Pipe", *Comb. and Flame*, **83**, pp.271-292
- Dimopoulos, P., Boulouchos, K. and Valentino, G. (1996). " Turbulent Flow Field Characteristics in a Reciprocating Engine: Appropriate cut-off Frequencies for Cycle-Resolved Turbulence, an analysis of Co-incident 3-D LDV Data Based on Combustion-Related Dimensional Arguments", 8th Intl. Symp. On Appl. Of Laser Techniques to Fluid Mechanics, July, 8th-11th, Lisbon Portugal
- Duarte, D., Ferrão, P and Heitor, M.V. (1997). "Turbulent Statistics and Scalar Transport in Highly-Sheared Premixed Flames", Proc. 11th Turbulent Shear Flows Symposium, Grenoble, 8-10 September
- Durst, F., Melling, A. and Whitelaw, J.H. (1981). "Principles and Practice of laser-Doppler Anemometry", Academic Press.
- Erdman, J.C. and Tropea, C.D. (1981). "Turbulence-induced Statistical in Laser Anemometers". Proc. 7th Biennial Symp. on Turbulence, Rolla, Missouri.

- Fernandes, E.C. (1998). "The Onset of Combustion Driven Acoustic Oscillations", Ph.D. Thesis, Instituto Superior Técnico, Lisbon-Portugal (in English)
- Fernandes, E.C., Ferrão, P., Heitor, M.V. and Moreira A.L.M (1994). "Velocity Temperature Correlation In Recirculating Flames With and Without Swirl", *Experimental Thermal and Fluid Science*, 9, pp.241-249
- Ferrão, P. and Heitor, M. V. (1998). "Probe and Optical Diagnostics for Scalar Measurements in Premixed Flames", *Experiments in Fluids*, 24, pp.389-398
- Ganji, A.R. and Sawyer, R.F. (1980). "Experimental Study of the Flowfield of a Two-Dimensional Premixed Turbulent Flame", *AIAA Journal*, Vol.18, no.7
- Gutmark, E., Parr, T.P., Hanson-Parr, D.M. and Schadow, K.C. (1989). "On the Role of Large and Small-Scale Structures in Combustion Control", *Combust. Sci. and Tech.*, 66, pp.107-126
- Gutmark, E., Schadow, K.C., Sivasegaram, S. and Whitelaw, J.H. (1991). "Interaction Between Fluid-Dynamic and Acoustic Instabilities in Combusting Flows Within Ducts", *Combust. Sci. and Tech.*, vol.79, pp. 161-166
- Hardalupas, Y., Tagawa, M. and Taylor, A.M.K.P (1996). "Characteristics of Counter-Gradient Heat Transfer in a Non Premixed Swirling Flame". In: Developments in Laser Techniques and Applications to Fluid Mechanics, ed. Durst et al., Springer-Verlag, pp. 159-184
- Heitor, M.V., Taylor, A.M.K.P. and Whitelaw, J.H. (1984). "Influence of Confinement on Combustion Instabilities of Premixed Flames Stabilised on Axisymmetric Baffles", *Combust. and Flame*, 57, pp. 109-121
- Heitor, M.V., Taylor, A.M.K.P. and Whitelaw, J.H. (1985). "Simultaneous Velocity and Temperature Measurements in a Premixed Flame". *Exp. in Fluids*, 3, pp. 323-339.
- Herzog, P., Valière, J.C., Valeau, V. and Tournois, G. (1996). "Acoustic Velocity Measurements by means of Laser Doppler Velocimetry", 8th Intl. Symp. On Appl. Of Laser Techniques to Fluid Mechanics, July, 8th-11th, Lisbon Portugal
- Hirt, F., Eisele, K., Zhang, Z. and Jud, E. (1996). "Pulsatile Flow Behaviour near Cardiac Prostheses Application and Limitation of Laser and MRI Techniques", 8th Intl. Symp. On Appl. Of Laser Techniques to Fluid Mechanics, July, 8th-11th, Lisbon Portugal
- Hussain, A.K.M.F. and Reynolds, W.C. (1970). "The Mechanics of an Organized Wave in Turbulent Shear Flow", *J. Fluid Mech.*, vol.41, part2, pp.241-258
- Hussain, A.K.M.F. and Zaman, K.B.M.Q. (1980). "Vortex Pairing in a Circular jet Under Controlled Excitation. Part 2. Coherent Structure Dynamics", *J. Fluid Mech.*, vol.101, pp.493-544
- Ishino, Y., Kojima, T., Oiwa, N. and Yamaguchi, S. (1996). "Acoustic Excitation of Diffusion Flames with Coherent Structure in a Plane Shear Layer", *JSME International Journal, series B*, Vol.39, no.1
- Keller, J.O. (1995). "Thermoacoustic oscillations in combustion chambers of gas turbine", *AIAA J.*, 33(12), pp.1125-1234.
- Keller, J.O. and Saito, .K. (1987). "Measurements of the Combusting Flow in a Pulse Combustor", *Combust.Sci. and Tech.*, 53, pp. 137-163
- Keller, J.O., Vaneveld, L., Korschelt, D., Hubbard, G.L., Ghoniem, A.F., Daily, J.W. and Oppenheim, A.K. (1982). "Mechanism of Instabilities in Turbulent Combustion Leading to Flashback", *AIAA Journal*, vol. 20, no.2
- Kiya, M. and Sasaki, K. (1985). "Structure of Large-Scale Vortices and Unsteady Reverse Flow in the Reattaching Zone of a Turbulent Separation Bubble", *J. Fluid Mech.*, vol. 154, pp.463-491
- Lang, W. and Vortmeyer, D. (1987). "Cross-correlation of sound pressure and heat release rate for oscillating flames with several frequencies excited", *Combust. Science and Tech.*, 54, pp. 399-406.

- Liou, T-M. and Santavicca, D.A. (1985). "Cycle Resolved LDV Measurements in a Motored IC Engine", Transactions of the ASME, Vol.107, pp232
- Lovett, J. A. and Turns, S. (1993). "The Structure of Pulsed Turbulent Nonpremixed Jet Flames", Combust. Sci. Tech, 94, pp. 193-217
- Schadow, K.C. and Gutmark, E. (1992). "Combustion instability related to vortex shedding in dump combustors and their passive control", Prog. Energy and Combust Science, 18, pp.117-132.
- Sivasegaram, S. and Whitelaw, J.H. (1987). " Oscillations in Confined Disk-Stabilized Flames", Comb. and Flame, 66, pp.121-129
- Tierderman, W.G., Privette, R.M. and Philipds, W.M. (1988). "Cycle-To-Cycle Variation Effects on Turbulent Shear Stress Measurements in Pulsatile Flows", Exp. in Fluids, 6, pp.265-272
- Witze, P.O. (1984). " Conditionally-Sampled Velocity and Turbulence Measurements in a Spark Ignition Engine", Combust. Sci. and Tech., vol.36,pp. 301-317
- Yanta, W.J. and Smith, R.A. (1978). "Measurements of Turbulent Transport Properties with a Laser Doppler velocimeter", 11th Aerospace Science Meeting, AIAA paper 73-169, Washington, USA
- Zhang, Z. Eisele, K. And Hirt, F. (1997). "The Influence of Phase-Averaging Window Size on the Determination of Turbulence Quantities in Unsteady Turbulent Flows", Experiments in Fluids, 22, pp.265-267.